Three-Dimensional Strong Langmuir Turbulence and Wave Collapse

P. A. Robinson, D. L. Newman, and M. V. Goldman
Department of Astrophysical, Planetary and Atmospheric Sciences, University of Colorado, Boulder, Colorado 80309
(Received 12 February 1988)

Results from the first fully three-dimensional simulations of driven damped strong Langmuir turbulence and wave collapse are presented. Key results are that turbulence is maintained at least in part by nucleation, the cores of most collapsing objects are pancake shaped in form, and the power spectrum falls off approximately as the product of a power law and an exponential at large wave number.

PACS numbers: 52.35.Ra, 52.35.Mw, 52.65.+z

The mechanisms of wave collapse and strong Langmuir turbulence have been investigated both at a fundamental level (see the articles by Goldman[1,2] and the references cited therein), and in connection with applications to the type-III events in the solar wind,[3] beams in the Earth's foreshock,[4] ionospheric modification,[5-7] beam-plasma experiments,[8,9] and inertial confinement fusion.[10] Since the original analysis by Zakharov,[11] much theoretical work on strong Langmuir turbulence has centered on the understanding of the late stages of the collapse of isolated wave packets,[1,2,11-14] while numerical calculations have been confined to one-dimensional (1D) and 2D systems or 3D cases under imposed spherical or axial symmetry. In reality, strong turbulence is intrinsically fully 3D in nature, has no spatial symmetry, and does not consist solely of isolated collapsing wave packets. Hence, it is of great interest to simulate fully three-dimensional turbulence directly.

In this study we present results from simulations of driven damped 3D strong turbulence. To our knowledge, these are the first such simulations to be carried out with good spectral and spatial resolution (on a 64^3 grid) and without any assumption of spherical or axial symmetry. The spatial and spectral structures of fully developed 3D turbulence are examined and comparisons are made between these results and those of calculations in 2D systems. Key results are the following: (i) The mechanism of nucleation in residual density cavities[15-17] is responsible, at least in part, for maintaining strong turbulence in the regimes investigated. (ii) The cores of collapsing wave packets are predominantly pancake shaped, rather than sausage shaped, a distinction that cannot be made on the basis of 2D simulations. (iii) Quadratic damping (in wave number k) is sufficient to halt collapse, whereas thermal Landau damping is not. (iv) The power spectrum has the form of the product of an exponential and a power law at large k.

Zakharov derived the following equations to describe strong electrostatic turbulence consisting of a mixture of Langmuir and ion sound waves[11]:

$$\nabla\cdot(i\partial_t+\nabla^2+i\hat{\gamma})\mathbf{E}=\nabla\cdot(n\mathbf{E}), \tag{1}$$

$$(\partial_t^2+2\hat{\alpha}\partial_t-\nabla^2)n=\nabla^2|\mathbf{E}|^2, \tag{2}$$

where $\mathbf{E}$, n, $\hat{\gamma}$, and $\hat{\alpha}$ are the Langmuir electric-field envelope, the particle density perturbation due to ion-sound waves, and the Langmuir and ion-sound damping operators, respectively. In these equations, length, time, n, and the electrostatic energy density $|\mathbf{E}|^2$ are dimensionless quantities, expressed in units of $(9m_i/4m_e)^{1/2}\lambda_{De}$, $3m_i/2m_e\omega_p$, $4m_en_0/3m_i$, and $4m_en_0k_BT_e/3m_i\epsilon_0$, respectively ($\epsilon_0$ is replaced by $1/4\pi$ in Gaussian units). The quantities m_e, m_i, λ_{De}, n_0, T_e, and ω_p are the electron mass, ion mass, Debye length, unperturbed ion density, electron temperature, and plasma frequency, respectively.

In the present work, Eqs. (1) and (2) are solved on a 64^3 grid of size $\approx(500\lambda_{De})^3$ [2D calculations use a 128^2 grid of size $\approx(1000\lambda_{De})^2$] with $m_i=1836m_e$. A spectral decomposition of the wave fields is employed, and is coupled with a semi-implicit predictor-corrector method to follow the time evolution of the spectral modes. The grids used are sufficiently large to ensure that the spatial periodicity implied by use of a spectral method does not induce any preferential alignment of the turbulent structures (e.g., parallel to the edges of the simulation volume), and aliasing effects are verified to be at an insignificant level. The system is weakly driven by negative Langmuir-wave damping centered at $k=0$, with $\gamma_{k=0}=-5.0\times10^{-4}\omega_p$. Negative damping gives way smoothly to power-law (positive) damping above $k\approx0.05k_{De}$, corresponding to ~400 driven modes. Power-law damping ($\gamma/\omega_p\approx2k^2/k_{De}^2$) is assumed, corresponding physically, for example, to the presence of a high-velocity power-law tail on the background plasma distribution. Such tails are commonly observed in the solar wind,[18] and are predicted to occur in strongly turbulent plasmas due to heating during wave collapse.[1,13,19] At large k, power-law damping is used to mimic the effect of transit-time damping[20] and is sufficiently strong to arrest 3D collapse.[16] We emphasize that, even in the presence of nonthermal damping, λ_{De} is defined unambiguously in terms of the assumed dispersion relation $\omega=\omega_p(1+3k^2\lambda_{De}^2/2)$, which leads to the dimensionless form (1) by means of the now standard rescaling (e.g., Ref. 1). The ion-sound damping is approximately of the form $|\mathrm{Im}(\omega_i)/\mathrm{Re}(\omega_i)|$

$=0.58$, with $\mathrm{Re}(\omega_i)=kc_s$ (ion sound speed $=c_s$). This (strong) damping corresponds to an electron/ion temperature ratio of $T_e/T_i=5$, which is appropriate for the physical situations mentioned above.

A central goal of strong-turbulence simulations has been to model fully developed 3D turbulence. Figure 1 shows Langmuir-wave packets and their associated density wells in a 3D turbulent state calculated under the conditions described above. This state is fully developed in the sense that, having been driven from an initial state consisting of low-level electrostatic noise, the simulation has been run for many ion-damping periods following a transient period dominated by modulational instabilities. Furthermore, apart from small fluctuations, the power spectra have become stationary with respect to time. A large number of randomly oriented collapsing wave packets and density wells are present in the simulation volume at any given time. Superposition of the two parts of the figure reveals that the wave packets and wells are not in one-to-one correspondence. This effect is due to ion inertia during the collapse and subsequent evolution: First, deepening of a well lags the increase in the electric field. Second, the electric field is observed to "burn out" at short scales, dissipating most of its energy via strong damping at large k. Third, the well tends to persist on the order of an ion time scale after the field has burned out.

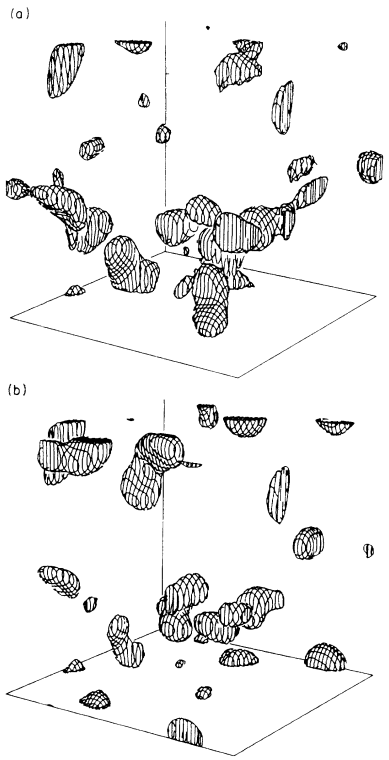

FIG. 1. Langmuir-wave packets and associated density wells in a state of 3D turbulence. (a) Surfaces of constant $|\mathbf{E}|^2$ are drawn surrounding the cores of collapsing wave packets at a level of 16% of the maximum value ($|\mathbf{E}|^2_{\max}=0.51n_0k_BT_e/\epsilon_0$) in the simulation volume. (b) Surfaces of constant $-n$ surrounding the cores of collapsing wave packets, drawn at 16% of the maximum ($-n_{\max}=0.13n_0$). The length of the box edge is $500\lambda_{De}$.

In 1D and 2D systems, the persistence of density wells after burnout has been found to favor near-resonant nucleation of new fields in these wells.[15-17] If this process plays a significant role in maintenance of the turbulence, the pairwise separations between collapses occurring within a given time interval should cluster toward smaller values than if their locations were randomly distributed. The cumulative distribution of pairwise, center-to-center separations x between collapses has been calculated in our simulations for a time interval containing 46 unambiguously identified collapses. Figure 2 shows the ratio of this probability distribution to the corresponding one calculated on the assumption that the collapses were randomly located. There is seen to be a strongly enhanced probability for separations between collapses to be small, indicating that nucleation plays a significant role in maintenance of 3D strong turbulence.

Examination of the cores of individual 3D collapsing wave packets shows that most are oblate (pancake shaped) during the early stages of collapse, rather than being prolate (sausage shaped). This result could not be inferred from 2D simulations, in which no such distinction is possible. In general, $-n$ and $|\mathbf{E}|^2$ are found to peak at the center of the wave packets, which have a typical aspect ratio of $\sim$2:1, in agreement with 2D simulations. One further observation is that strong damping at high k tends to remove short-scale structures, and can reduce the eccentricity of the wave packet as collapse proceeds into its final stages. Figure 3 shows the core of a 3D wave packet at 3 times during the early stages of its collapse. Surfaces of constant $|\mathbf{E}|^2$ are drawn at 64% of the instantaneous maximum at the center of the

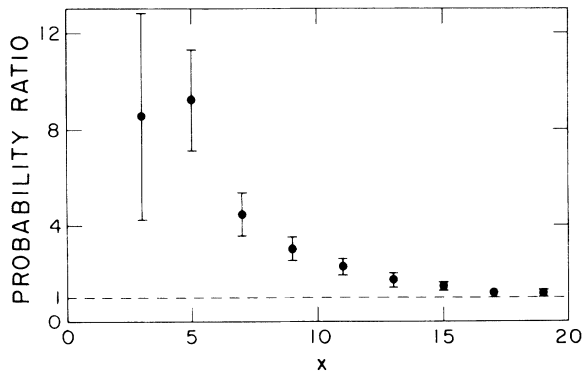

FIG. 2. Ratio of the cumulative probability of the separation between collapses x (in grid spacings) to the corresponding probability for uncorrelated collapses. Statistics are compiled from all pairwise separations between 46 consecutive events in fully developed 3D turbulence.

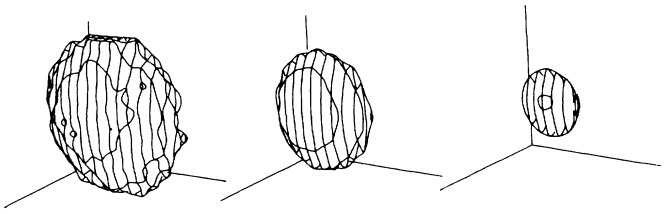

FIG. 3. Collapse of the core of a 3D Langmuir-wave packet. A surface of constant $|\mathbf{E}|^2$ is drawn at a level of 64% of the central maximum in each case. Each frame has edge length $\approx 80\lambda_{De}$ and shows $\frac{1}{8}$ of the simulation volume, centered on the wave packet.

wave packet. These pancake-shaped surfaces are seen to contract as the collapse proceeds, while maintaining their oblate form. The axis of (approximate) symmetry of an individual collapsing wave packet is determined by the precise conditions at the time of its formation, since the driving and damping are isotropic. The collapsing wave packets in the resulting ensemble are randomly oriented and hence the turbulence is isotropic.

The time-averaged (over an interval containing many collapses), angle-integrated electrostatic energy and dissipation spectra of 3D turbulences are shown in Fig. 4. The main features are shared by both the 3D spectra and their 2D counterparts: Except at the smallest k, the energy spectra behave approximately as $|E_{\mathbf{k}}|^2 \sim \exp(-ak)/k^{2d-2}$, where a is a constant and d the dimension. The density spectra show similar behavior, with $n_{\mathbf{k}} \sim \exp(-bk)/k^{d-1}$, where b is a constant. Qualitatively similar spectra (power law, becoming exponentially small at large k) have been theoretically predicted under specific assumptions concerning the damping and self-similarity of collapse.[1,13,21] The 2D and 3D dissipation spectra are also quite similar, with driving at small k and a dissipation peak at $k \approx 0.1 k_{De}$. There is essentially no inertial range.[22] Theory implies that damping must increase at least as fast as $k^{d/2}$ at large k to arrest collapse before an unphysical singularity develops.[15] Our results agree with this prediction insofar as we have found that k^2 damping is sufficient to halt collapse in 3D and (in other simulations) that thermal Landau damping ($\sim k \ln k$ at large k) appears to be insufficient.

In summary, fully developed 3D strong turbulence has the following key features in the regimes investigated: (i) It is maintained, at least in part, by nucleation. (ii) The collapsing wave packets are predominantly oblate. (iii) Its energy spectrum falls off approximately as the product of a power law and an exponential function at large k. (iv) Its energy and dissipation spectra are similar to the 2D case. (v) Thermal Landau damping appears to be too weak to halt collapse in 3D, whereas k^2 damping is sufficient. In future work, we will investigate the dynamical and statistical features of 3D turbulence in detail, including the connection between the theory of

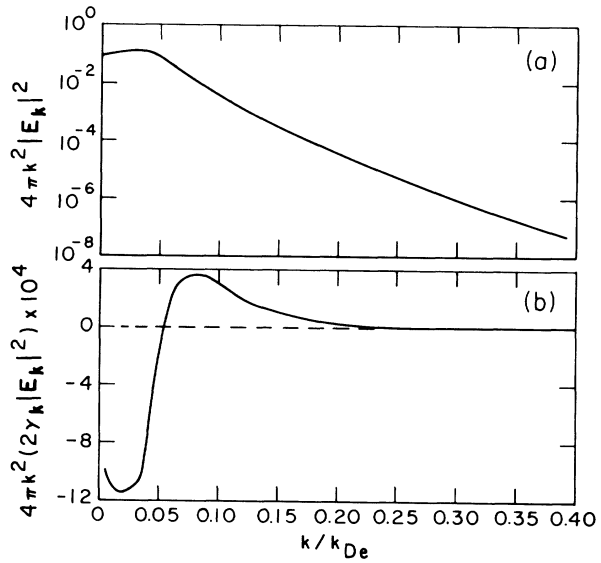

FIG. 4. Angle-interpreted energy and dissipation spectra for 3D strong turbulence. (a) Energy spectrum: $4\pi k^2|\mathbf{E}_{\mathbf{k}}|^2$. (b) Dissipation spectrum: $8\pi k^2\gamma_{\mathbf{k}}|\mathbf{E}_{\mathbf{k}}|^2$. Here, k, $|\mathbf{E}|^2$, and $\gamma_{\mathbf{k}}$ are measured in units of k_{De}, $n_0 k_B T_e/\epsilon_0$, and ω_p, respectively.

isolated collapsing wave packet and those actually observed in simulations, the dependence of energy and dissipation spectra on the damping and the existence or otherwise of an inertial range, and the role of nucleation in maintenance of the turbulent state.

This work was supported by the National Science Foundation's Solar-Terrestrial Division and NASA's Solar Terrestrial Theory and Solar Heliospheric Programs under Grants No. ATM-8511906, No. NAGW-91, and No. NSG-7287, respectively, to the University of Colorado at Boulder. The computations were carried out at the National Center for Atmospheric Research.

[1]M. V. Goldman, Rev. Mod. Phys. **56**, 709 (1984).
[2]M. V. Goldman, Physica (Amsterdam) **18D**, 67 (1986).
[3]M. V. Goldman, Solar Phys. **89**, 403 (1983).
[4]D. L. Newman, Ph.D. thesis, University of Colarado, Boulder, Colorado, 1985 (unpublished).
[5]J. P. Sheerin, J. C. Weatherall, D. R. Nicholson, G. L. Payne, M. V. Goldman, and P. J. Hansen, J. Atmos. Terr. Phys. **44**, 1043 (1982).
[6]W. Birkmayer, T. Hagfors, and W. Kofman, Phys. Rev. Lett. **57**, 1008 (1986).
[7]A. Y. Wong, T. Tanikawa, and A. Kuthi, Phys. Rev. Lett. **58**, 1375 (1987).
[8]H. C. Kim, R. L. Stenzel, and A. Y. Wong, Phys. Rev. Lett. **33**, 886 (1974).
[9]A. Y. Wong and P. Y. Cheung, Phys. Rev. Lett. **52**, 1222 (1984).
[10]H. A. Rose, D. F. DuBois, and B. Bezzerides, Phys. Rev.

Lett. **58**, 2547 (1987).

[11]V. E. Zakharov, Zh. Eksp. Teor. Fiz. **62**, 482 (1972) [Sov. Phys. JETP **35**, 908 (1972)].

[12]L. M. Degtyarev, V. E. Zakharov, and L. I. Rudakov, Fiz. Plazmy, **2**, 438 (1976) [Sov. J. Plasma Phys. **2**, 240 (1976)].

[13]G. Pelletier, Phys. Rev. Lett. **49**, 782 (1982).

[14]G. Pelletier, Physica (Amsterdam) **27D**, 187 (1987).

[15]G. D. Doolen, D. F. DuBois, and H. A. Rose, Phys. Rev. Lett. **54**, 804 (1985).

[16]D. Russell, D. F. DuBois, and H. A. Rose, Phys. Rev. Lett. **56**, 838 (1986).

[17]D. Russell, D. F. DuBois, and H. A. Rose, to be published.

[18]R. P. Lin, Space Sci. Rev. **16**, 189 (1974).

[19]A. A. Galeev, R. Z. Sagdeev, V. D. Shapiro, and V. I. Sevchenko, Fiz. Plazmy **1**, 10 (1975) [Sov. J. Plasma Phys. **1**, 5 (1975)].

[20]V. B. Rozanov and S. A. Shumskiĭ, Kvantovaya Elektron. (Moscow) **13**, 1545 (1986) [Sov. J. Quantum Electron. **16**, 1010 (1986)].

[21]M. V. Goldman and G. Pelletier, in Proceedings of the Workshop on Nonlinear Radio Frequency Excitation of the Ionosphere, Fairbanks, Alaska, August 1987 (to be published).

[22]J. C. Weatherall, D. R. Nicholson, and M. V. Goldman, Phys. Fluids **26**, 1103 (1983).